**Journal of Petroleum Research and Studies**

**Open Access**
**Vol. 14, No. 4, December 2024, pp. 154-169**

**P- ISSN: 2220-5381**
**E- ISSN: 2710-1096**

DOI: http://doi.org/10.52716/jprs.v14i4.899

# Experimental Investigation of a Regenerative Kalina Cycle for Electrical Power Generation Using Waste Heat

**Abdulkhodor K. Nassir[*1], Haroun A. K. Shahad[1,2]**

[1]College of Engineering, Mechanical Engineering Department, University of Babylon, Babylon, Iraq.

[2]College of Engineering Technologies, University of Hilla, Babylon, Iraq.

[*]Corresponding Author E-mail: alhaji84@yahoo.com

Received 04/01/2024, Revised 04/06/2024, Accepted 09/06/2024, Published 22/12/2024



## Abstract

Kalina cycle is a thermodynamic power cycle uses any waste heat source (low temperature source) to generate electrical power or cooling. Many versions of Kalina cycle exist. In this paper a regenerative Kalina version is designed and constructed. The cycle consists of the following main components: heat recovery vapor generator (HRVG), separator, turbine, condenser, throttling valve, mixer (absorber), heat exchanger and pump. The heat exchanger is used to heat the working fluid coming from the pump before entering the HRVG by the hot saturated liquid (weak solution) coming from the separator. The cycle uses aqua ammonia mixture as the working fluid with different ammonia concentrations. The effect of many operating conditions on cycle performance is studied such as ammonia ($NH_3$) mass fraction (range from 0.85-0.89), low pressure (range from 2-4 bar), and maximum pressure (range from 20-40 bar). The dryness fraction (DF) at separator entrance is kept at 0.3. The results show that the highest thermal efficiency obtained is 12.9% at $P_{max}$=35 bar, $P_{min}$=2 bar, and x=0.85. The highest value of the net power is 0.367 kW at x=0.89 at turbine inlet pressure of $P_{max}$=20 bar. The highest value of exergy efficiency is 28.5% at $P_{max}$=35 bar, $P_{min}$=2 bar. It is noticed that the highest exergy destruction is in the heat recovery vapor generator (HRVG) which is about 48% due to high temperature heat exchange process and low mass flow rate. The exergy destruction is larger at $P_{max}$=35 and x=0.89 than the exergy destruction at $P_{max}$=20 bar and x=0.89.

**Keywords:** Kalina cycle, waste heat source, aqua-ammonia, heat recovery vapor generator, exergy efficiency.

Journal of Petroleum Research and Studies

Open Access
Vol. 14, No. 4, December 2024, pp. 154-169

P- ISSN: 2220-5381
E- ISSN: 2710-1096

# دراسة عملية لدورة كالينا التوليدية لإنتاج القدرة الكهربائية من الحرارة الضائعة

**الخلاصة:**

دورة كالينا احدى الدورات الثرموديناميكية وهي تستخدم لتوليد القدرة الكهربائية من الحرارة الضائعة في مصادر الطاقة ذات درجات الحرارة الواطئة مثل غازات نواتج الاحتراق وحرارة باطن الارض والطاقة الشمسة .....الخ. توجد عدة تصاميم لدورة كالينا تعتمد على عدد المبادلات الحرارية ومائع الشغل المستخدم والظروف التشغيلية. تم في هذا البحث تصميم وبناء محطة توليد قدرة كهربائية تعمل بنسخة مطورة من دورة كالينا. تتكون هذه الدورة من المكونات التالية: مولد البخار مسترجع الحرارة – الفاصل – التوربين – الخلاط والماص – صمام الخنق- المكثف- والمضخة. يستخدم في المحطة خليط الماء والامونيا كمائع للشغل. تم اضافة مبادل حراري لتسخين مائع الشغل القادم من المضخة قبل دخوله الى مولد البخار بواسطة الحرارة المسحوبة من المائع الشبع الحار( قليل الامونيا) القادم من الفاصل. تم تغيير تركيز الامونيا في المائع عند مدخل التوربين (0.85-0.89) لدراسة تأثير التركيز على اداء المحطة. كذلك تم دراسة تأثير تغير اعلى ضغط (20-40 bar) واقل ضغط (2-4 bar) على اداء المحطة. اما كسر جفاف البخار عند مدخل الفاصل فقد تم تثبيته عند قيمة (0.3). اظهرت نتائج الدراسة انه تم الحصول على اعلى كفاءة للدورة (12.9%) عند الظروف التشغيلية: اعلى ضغط (35 bar) اقل ضغط (2 bar) وتركيز امونيا عند مدخل التوربين (0.85). أما اقصى قدرة (0.367 kW) فقد تم الحصول عليها عند الظروف التشغيلية: اقصى ضغط (20bar) واقل ضغط (2 bar) وتركيز امونيا عند مدخل التربين (0.89). أما اقصى كفاءة اكسيرجية وهي (28.5%) فقد تم الحصول عليها عند الظروف التشغيلية: اقصى ضغط (35 bar) واقل ضغط (2 bar) وتركيز امونيا عند مدخل التوربين (0.85). كذلك اظهرت النتائج ان اكبر خسارة اكسيرجية كانت في مولد البخار وتبلغ (48%) وان الخسائر الاكسيرجية تزداد كلما زاد أقصى ضغط.

## 1. Introduction:

Nowadays, as energy demand and fossil fuel consumption rise, so too does pollution. Due to limited conventional energy resources, much research has focused on developing new energy sources and reducing pollution and costs. The Kalina cycle recovers heat from low-grade sources and converts it into useful work and electricity. This helps decrease fossil fuel use and associated emissions. Two Kalina cycle systems, KCS1 and KCS34, for cogenerating power from waste heat in cement plants. Optimization showed KCS1 had an efficiency of 22.9% and KCS34 had 21.9%. Exergy efficiencies were 55.8% for KCS1 and 53.2% for KCS34 [1]. The examination of the effect of two turbines on Kalina system performance, aiming to increase power output and efficiency. Using two expansion turbines boosted efficiency 4.04% over a single turbine system, reaching a maximum of 28.7% at 35 bar intermediate pressure. In summary, the Kalina cycle enables effective low-grade heat recovery for useful electricity generation while reducing fossil fuel consumption and emissions. Adding a second turbine further improves power output and efficiency [2].

The turbine inlet temperature, pressure, separator pressure, and ammonia mass fraction affect a modified Kalina power-cooling cycle. Energy efficiency rose from 13.82% to 16.39%, while COP went from 0.59 to 0.75 [3]. The using of solar pond heat for cogenerating electricity and

Open Access
Vol. 14, No. 4, December 2024, pp. 154-169
P- ISSN: 2220-5381
E- ISSN: 2710-1096

fresh water. Capturing heat from a salinity-gradient solar pond can produce outstanding results for residential needs. Theoretical analysis of two systems driven by a solar pond was done to cogenerate fresh water and power by integrating Rankine or Kalina cycles with reverse osmosis desalination. Simulations showed the solar pond-Rankine/RO system provided 4 $m^3$/h of fresh water and 29.6 kW of electricity using R600a. Meanwhile, the solar pond-Kalina/RO system produced 3.3 m3/h of fresh water and 15.5 kW of electricity. In summary, the Kalina cycle can effectively utilize low-grade heat sources like solar ponds to cogenerate fresh water and electricity [4].

The investigation of cogenerating hydrogen and fresh water from geothermal heat, using an exergoeconomic analysis. The system comprised a Kalina cycle, humidification-dehumidification, thermoelectric generators, and proton exchange membrane electrolysis [5]. The proposing of cogenerating power and distilled water from stored solar pond heat. Their system used a Kalina cycle, humidification-dehumidification, and thermoelectrics with a solar pond. Multi-objective optimization increased energy utilization, exergy efficiency, and reduced costs [6]. The studying two modified Kalina cycles, adding a multiphase expander. This boosted net power 3.23% and efficiency 3.68% in one version. In summary, the Kalina cycle can effectively utilize geothermal and solar pond heat sources to cogenerate useful products like hydrogen, fresh water, and power through system modifications like adding expanders. Exergoeconomic analysis helps optimize these systems [7].

The comparison of Kalina and organic Rankine cycles using geothermal heat, with water flow rates from 120 to 550 m3/h and temperatures up to 86°C. The Kalina cycle produced about 40% more gross power, though both had similar thermal efficiencies around 6.49% [8]. The investigatation a biomass-fired Kalina system with a regenerative heater to boost feedwater temperature and efficiency, like in coal power plants. Thermodynamic analysis of the biomass-fired Kalina cycle with regeneration showed higher turbine inlet pressures and temperatures increased net power and efficiency, while raising separator inlet temperature. The boiler had the most exergy destruction at 88%, versus 3% in the turbine and 8.5% in heat exchangers. In summary, the Kalina cycle can effectively utilize low-temperature geothermal and biomass heat sources. Regenerative heating further improves the efficiency. The boiler causes the most exergy destruction [9].

The analyzing of Organic Rankine and Kalina cycles to produce electricity from geothermal sources at 82°C and 51.22 kg/s flow. The ORC generated up to 0.24 MW and 940 MWh. The

Open Access
Vol. 14, No. 4, December 2024, pp. 154-169
P- ISSN: 2220-5381
E- ISSN: 2710-1096

Kalina cycle produced up to 0.43 MW and 1730 MWh, almost double [10]. The examinationof a KCS using solid waste heat from a Turkish power plant, recovering 0.9546 MW at 24.15% thermal efficiency [11]. The investigatation of combining Kalina and organic Rankine cycles to recover 450°C, 2 kg/s exhaust heat from a waste recycling factory's CHP engine. The combined cycle produced 211.03 kW net power at 52.83% exergy efficiency and 26.50% thermal efficiency, with a 4.2-year payback. In summary, Kalina cycles can effectively utilize low-grade industrial waste heat, outperforming organic Rankine cycles. Heat recovery to the Kalina cycle from solid waste and exhaust gases can produce useful electricity at reasonable efficiency and payback [12].

Nassir and Shahad [13]analyzed a simple Kalina cycle (SKCS) and modified Kalina cycle (MKCS) using low temperature sources and an ammonia-water working fluid. Adding a heat exchanger in the MKCS boosted efficiency 33.6% and power 27.8% over the SKCS. Maximum efficiencies reached 14.7% for the MKCS and 0.5641 kW net power, with exergy efficiencies of 24.8% for the MKCS versus 11.7% for the SKCS. In another study [13], The comparison of the SKCS to two MKCS versions using additional heat exchangers. The two-heat-exchanger MKCS2 achieved a maximum thermal efficiency of 18.85%, versus 12.7% for the MKCS1 and 8.64% for the SKCS [14].

The analyzing of Iraq's geothermal potential, finding no significant high-temperature sources but possibilities for low-temperature applications using depleted petroleum wells.

In this work, an experimental regenerative Kalina cycle system is constructed and tested. The cycle's performance is studied under different ammonia mass fractions, maximum pressures, and minimum pressures [15].

## 2. Experimental Work

### 2.1 Cycle Components

The modified Kalina cycle system studied here consists of a heat recovery vapor generator (HRVG), separator, turbine, heat exchanger, throttling valve, mixer (absorber), condenser, main tank and pump, as shown in Figure (1). This is a modification of the simple Kalina cycle, with a heat exchanger added between the separator and throttling valve. This recovers heat from the weak separator solution to preheat the working fluid from the pump before the HRVG.

In the regenerative Kalina cycle, the working fluid enters the separator as wet vapor (point 7). The vapor phase (point 8) expands in the turbine to generate power. The weak separator solution

Open Access
Vol. 14, No. 4, December 2024, pp. 154-169
P- ISSN: 2220-5381
E- ISSN: 2710-1096

(point 9) exchanges heat in the regenerative heat exchanger. The throttle valve reduces the pressure of the cooled weak solution (point 10) before mixing with the turbine exhaust (point 11) in the absorber. The strong solution from the absorber (point 12) is pumped to the regenerative heat exchanger (point 5) to recover heat from the weak solution. The preheated working fluid (point 6) enters the HRVG where heat is supplied to generate wet vapor again, completing the cycle. The wet vapor separates into two parts in the separator, strong solution (saturated vapor) and weak solution (saturated liquid). The strong solution enters the turbine (point 1). At the turbine entrance the quality of the vapor is saturated vapor at maximum pressure. Then the saturated vapor expands in the turbine and leaves as a wet vapor (point 2). The weak solution enters the heat exchanger as saturated liquid at maximum pressure (point 8) and leaves the heat exchanger at (point 8̀). The working fluid enters the heat exchanger at (point 5) as sub cool with maximum pressure and it leaves from point 5̀. The weak solution inters the throttling valve (point 8̀) as saturated liquid and leaves it as a wet vapor (point 9). The strong solution (point 2) and the weak solution (point 9) are mixed in the mixer-absorber and the solution leaves the as wet vapor at minimum pressure (point 3). After that the solution enters the condenser and leaves as a saturated liquid (point 4). The solution is pumped back to the heat exchanger as subcooled liquid at maximum pressure to enter the HRVG, (point 5̀) and heated to (point 6) which is less than the boiling temperature of the working fluid at maximum pressure. The solution leaves the HRVG as wet vapor at maximum pressure point 7 to complete the cycle as shown in Figure (2).

### 2.2 Design assumptions

1. Steady state operation.
2. Constant HRVG and condenser pressures.
3. Constant separator and mixer pressures and temperatures.
4. Isenthalpic throttling.
5. 100% pump efficiency, 85% turbine efficiency.
6. 0.91 coupling efficiency.
7. Negligible pressure/heat/friction losses.
8. 100% HRVG and condenser effectiveness.
9. Adiabatic components except mixer.
10. Kinetic/potential energy changes neglected.
11. Pure ammonia-water working fluid.

Open Access
Vol. 14, No. 4, December 2024, pp. 154-169
P- ISSN: 2220-5381
E- ISSN: 2710-1096

12. 175°C hot gas inlet temperature.
13. Turbine inlet at turbine pressure saturation temperature.
14. 20°C HRVG pinch point.
15. 15°C HRVG terminal temperature difference.
16. 2°C HRVG approach point.
17. Defined working fluid qualities at key cycle points.

In summary, key simplifying assumptions are made including constant pressures, 100% component effectiveness, adiabatic components, and defined temperature differences. Pure ammonia-water working fluid is assumed and flow losses are neglected. Defined fluid qualities are specified at key cycle points.

**Table (1) The Situation of the Fluid during the Cycle**

| Point | Situation |
|---|---|
| 1 | Saturated vapor mixture (strong solution) |
| 2 | Wet vapor mixture (strong solution) |
| 3 | Wet vapor mixture (working fluid) |
| 4 | Saturated liquid (working fluid) |
| 5 | Sub-cool liquid (working fluid) |
| 5̀ | Warm liquid (working fluid) |
| 6 | Hot liquid (working fluid) |
| 7 | Wet vapor (working fluid |
| 8 | Saturated liquid mixture (hot weak solution) |
| 8̀ | Saturated liquid mixture (warm weak solution) |
| 9 | Saturated liquid mixture (warm weak solution) |

Open Access
Vol. 14, No. 4, December 2024, pp. 154-169

P- ISSN: 2220-5381
E- ISSN: 2710-1096

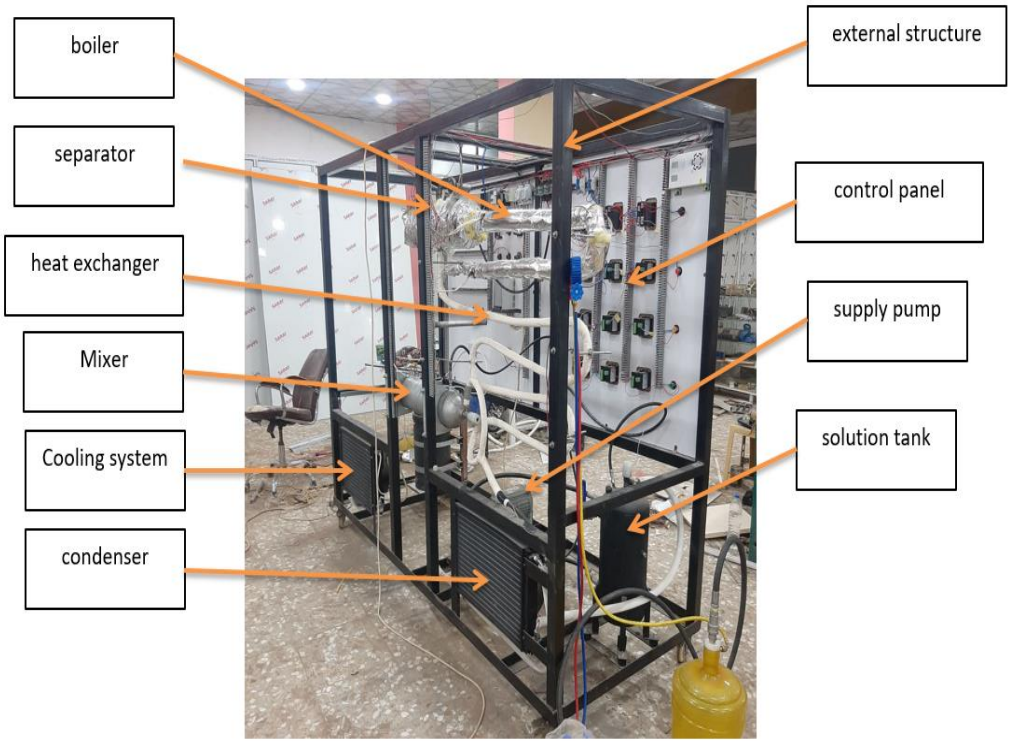


**Fig. (1): Experimental Regeneration Kalina Cycle (RGKCS)**

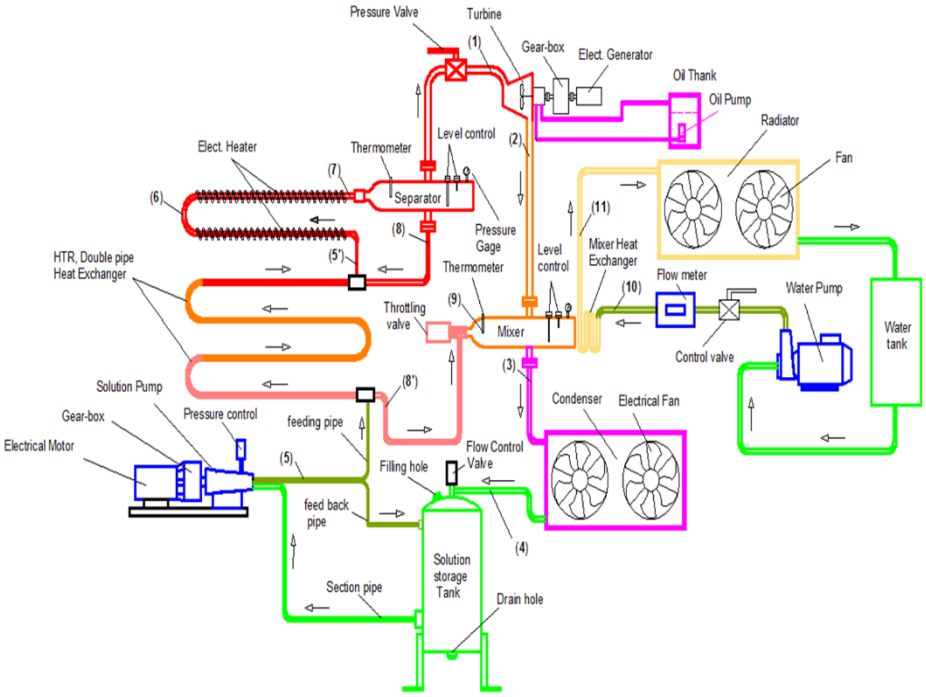


**Fig. (2): Schematic Diagram of (RGKCS)**

Open Access
Vol. 14, No. 4, December 2024, pp. 154-169
P- ISSN: 2220-5381
E- ISSN: 2710-1096

### 2.3 Governor Equations

The thermodynamic analysis of the Kalina cycle utilizes mass, energy, and exergy conservation equations for each component. The exergy analysis is conducted under the same general assumptions. The exergy rate of each fluid stream is calculated as: [14].

$$\sum \dot{m}_i = \sum \dot{m}_o \quad (1)$$

$$\sum \dot{m}_i x_i = \sum \dot{m}_o x_o \quad (2)$$

$$\sum \dot{Q} + \sum \dot{m}_i h_i = \sum \dot{W} + \sum \dot{m}_o h_o \quad (3)$$

$$\dot{E}_{dtot} = \sum \dot{E}_{in} - \sum \dot{E}_{out} \quad (4)$$

$$(\dot{E}_d)_{tot} = \sum (\dot{E}_d)_i \quad (5)$$

$$\eta_{ex} = \frac{\dot{W}_{net}}{(\dot{E}_{in} - \dot{E}_{out})_{H.G}} \quad (6)$$

$$\dot{E} = \dot{m}(h - T_0 s) \quad (7)$$

$$\eta_{th} = \frac{\dot{W}_{net}}{\dot{Q}_{in}} = \frac{\dot{W}_T - \dot{W}_P}{\dot{Q}_{in}} \quad (8)$$

## 3. Results and Discussions

This section presents and discusses the experimental results for the regenerative Kalina cycle system. The performance parameters analyzed include thermal efficiency, net power output, exergy efficiency, and exergy destruction. The effects of varying ammonia mass fraction, maximum cycle pressure, and minimum cycle pressure are examined.

The maximum pressure is varied from 20 bar to 40 bar in 5 bar increments. The minimum pressure is varied between 2 bar, 3 bar, and 4 bar. The ammonia mass fraction ranges from 0.85 to 0.89 in 0.01 increments. The separator inlet dryness fraction is held constant at 0.3.

Heat is supplied by an electrical heater with power of 1000-4000 W. The results provide insights into how these key parameters influence the thermodynamic performance of the cycle. The exergy analysis quantifies the sources of irreversibility under the tested conditions.

### 3.1 Effect of ammonia mass fraction

Figures (3, 4, and 5) show the relationship between the ammonia mass fraction and the thermal efficiency with different maximum pressures at constant minimum pressure and dryness fraction.

Open Access
Vol. 14, No. 4, December 2024, pp. 154-169

P- ISSN: 2220-5381
E- ISSN: 2710-1096

All the figures show same trend for all cases. When the ammonia mass fraction increases the efficiency decreases at constant maximum pressure because of the increasing of the mass flow rate. The highest thermal efficiency is 12.9% at $P_{max}$=35 bar, $P_{min}$=2 bar, DF=0.3 and x=0.85. The lowest thermal efficiency is 6.8% at $P_{max}$=20 bar, $P_{min}$=4 bar, DF=0.3 and x=0.89 because at these conditions high mass flow rate and high minimum pressure.

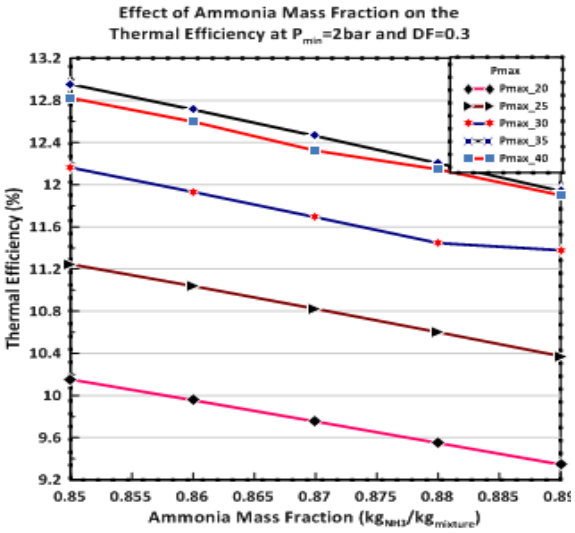


**Fig. (3): Effect of ammonia mass fraction on thermal efficiency of RGKCS at $P_{min}$=2 bar and DF=0.3**

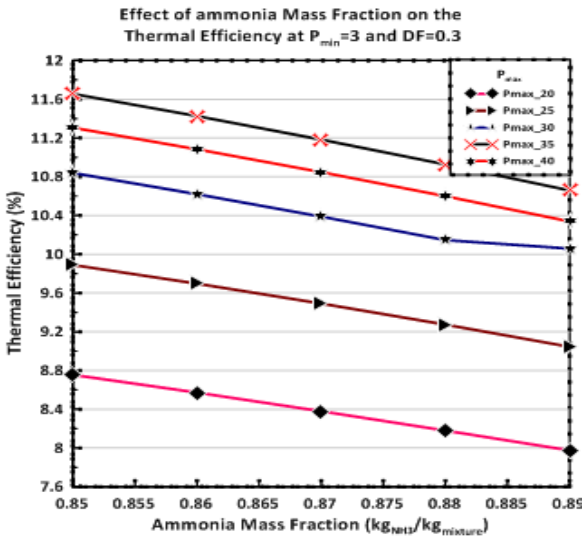


**Fig. (4): Effect of ammonia mass fraction on thermal efficiency of RGKCS at $P_{min}$=3 bar and DF=0.3**

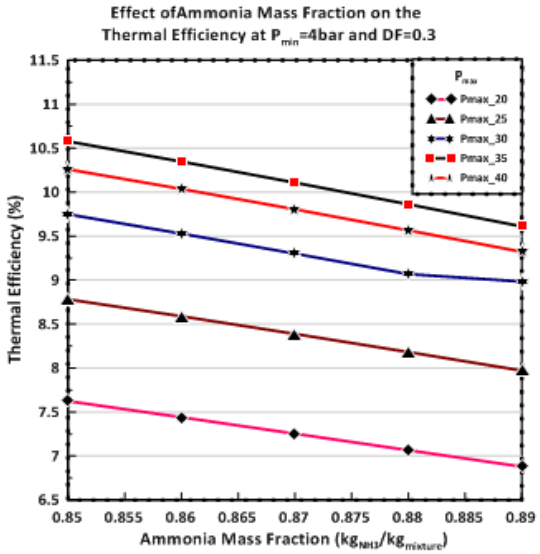


**Fig. (5): Effect of ammonia mass fraction on thermal efficiency of RGKCS at $P_{min}$=4 bar and DF=0.3**

Open Access
Vol. 14, No. 4, December 2024, pp. 154-169
P- ISSN: 2220-5381
E- ISSN: 2710-1096

Figures (6, 7, and 8) display the effect of the ammonia mass fraction on the net power. The highest value of the net power is 0.367 kW at x=0.89 at turbine inlet, $P_{max}$=20 bar and DF=0.3 at separator inlet. When the ammonia mass fraction increases the net power increases. Since the increase in ammonia mass fraction increases the vapor mass flow rate through the turbine, which increases the power output. The lowest value of the net power is obtained at x=0.85 because in this ammonia mass fraction has low mass flow rate.

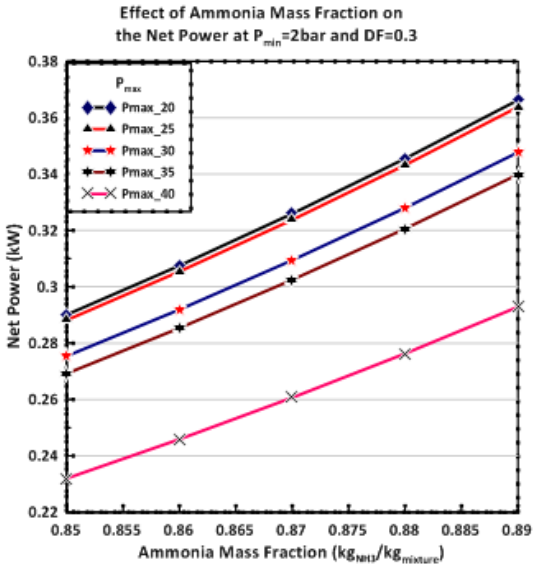


**Fig. (6): Effect of ammonia mass fraction on net power of RGKCS at $P_{min}$=2 bar and DF=0.3**

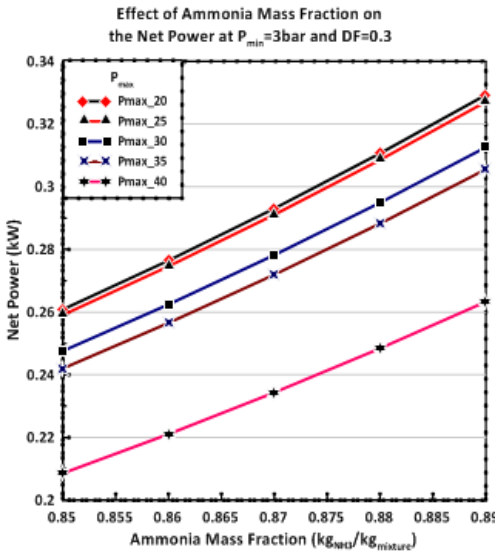


**Fig. (7): Effect of ammonia mass fraction on net power of RGKCS at $P_{min}$=3 bar and DF=0.3**

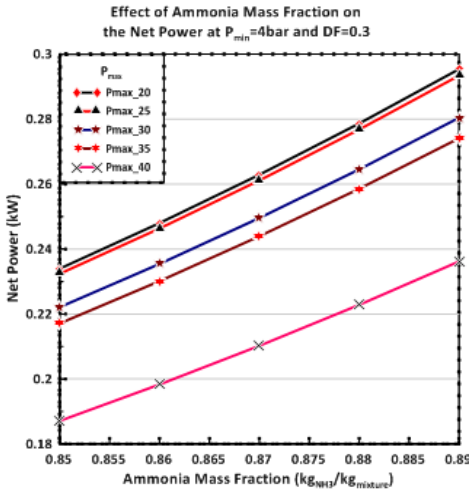


**Fig. (8) Effect of ammonia mass fraction on net power of RGKCS at $P_{min}$=4 bar and**

Open Access
Vol. 14, No. 4, December 2024, pp. 154-169
P- ISSN: 2220-5381
E- ISSN: 2710-1096

**DF=0.3**

Figures (9, 10, and 11) display the relationship between the ammonia mass fraction and the exergy efficiency. When the ammonia mass fraction increases the exergy efficiency drops due to the increase in mass flow rate same as mentioned before. Hence the exergy destraction increases that's lead to drop the exergy efficiency. This is the same behavior as the thermal efficiency. The highest value of exergy efficiency is 28.5% at $P_{max}$=35 bar, $P_{min}$=2 bar and DF=0.3. It is noticed the minimum value of exergy efficiency is 15% at $P_{max}$=20 bar, $P_{min}$=4bar and x=0.89.

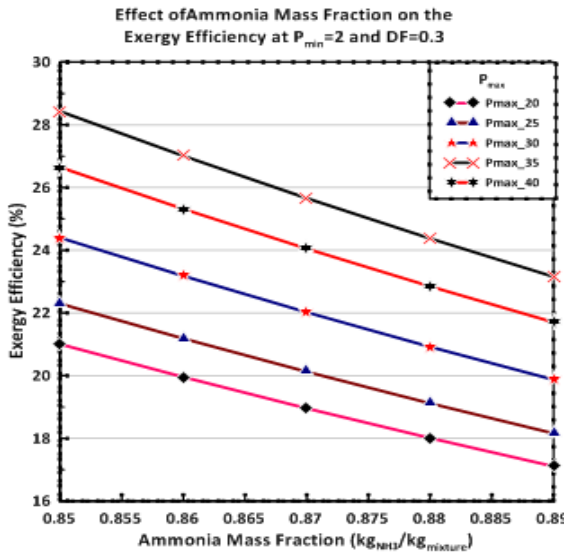


**Fig. (9): Effect of ammonia mass fraction on exergy efficiency of RGKCS at $P_{min}$=2 bar and DF=0.3**

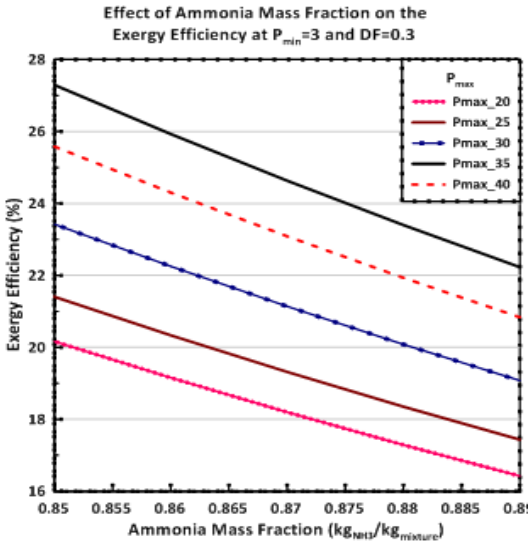


**Fig. (10): Effect of ammonia mass fraction on exergy efficiency of RGKCS at $P_{min}$=3 bar and DF=0.3**

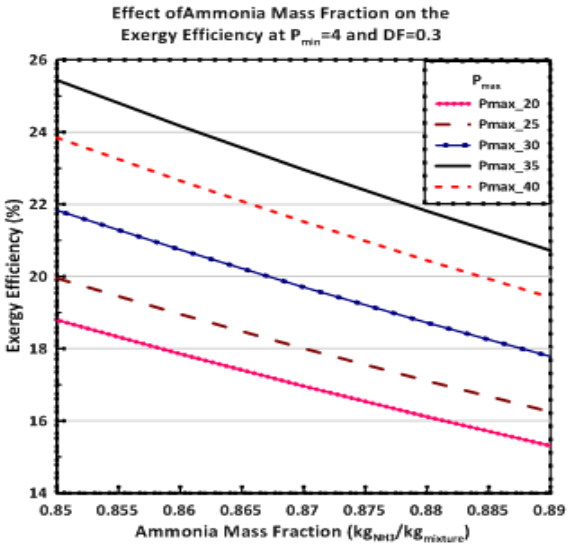


**Fig. (11): Effect of ammonia mass fraction on exergy efficiency of RGKCS at $P_{min}$=4 bar and DF=0.3**

Open Access
Vol. 14, No. 4, December 2024, pp. 154-169
P- ISSN: 2220-5381
E- ISSN: 2710-1096

## 3. Exergy Destruction

Figure (12) shows the exergy destruction in each component. It is noticed that the highest exergy destruction is in the heat recovery vapor generator (HRVG) which is about 48% because the low mass flow rate which pass through the HRVG that lead to more loses in the HRVG and also heat transfer devices produce more exergy destruction. It may be due to the heigher temperature at which is heat is exchanged. The second component which has more loses is the condenser has 17% from the exergy destruction. The hot working fluid should be cooled in the condenser that is loses. The other loses are in the absorber, separator and heat exchanger are 12%, 9% and 8% respectively. The exergy destruction in the pump and the throttling valve is 1% because the temperature doesn't drop too much.

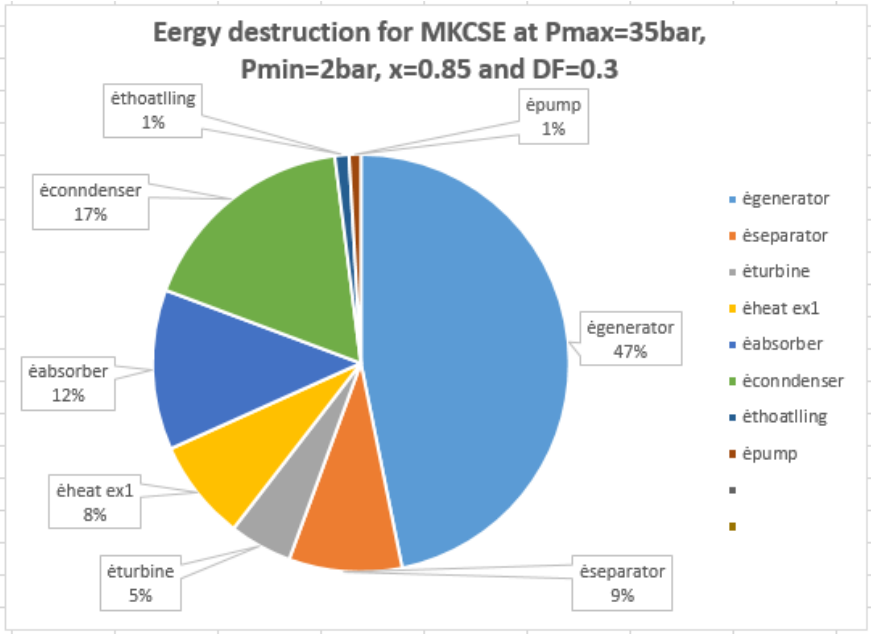


**Fig. (12): Exergy destruction in RGKCS at Pmax=35 bar, Pmin=2 bar, x=0.85 and DF=0.3**

Figures (13) and (14) show the effect of ammonia mass fraction on exergy destruction in the cycle for different minimum pressure at maximum pressure. The dryness fraction is kept constant in both figures at 0.3. It is seen that the exergy destruction increases with the increasing ammonia mass fraction in the solution due to the increasing in the circulate rate throughout the cycle. The exergy destruction in $P_{max}$=35 and x=0.89 is larger than the exergy destruction at $P_{max}$=20 bar and x=0.89 because the net power at $P_{max}$=20 bar is higher than the net power at $P_{max}$=35 bar. As mention at section 5.2.2 when the maximum pressure increases the mass flow rate decreases.

Open Access
Vol. 14, No. 4, December 2024, pp. 154-169

P- ISSN: 2220-5381
E- ISSN: 2710-1096

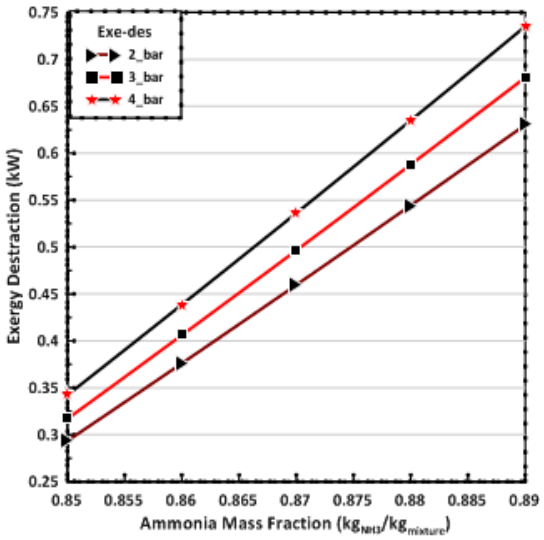


**Fig. (13): Exergy destruction of RGKCS at Pmax=20 bar and DF=0.3**

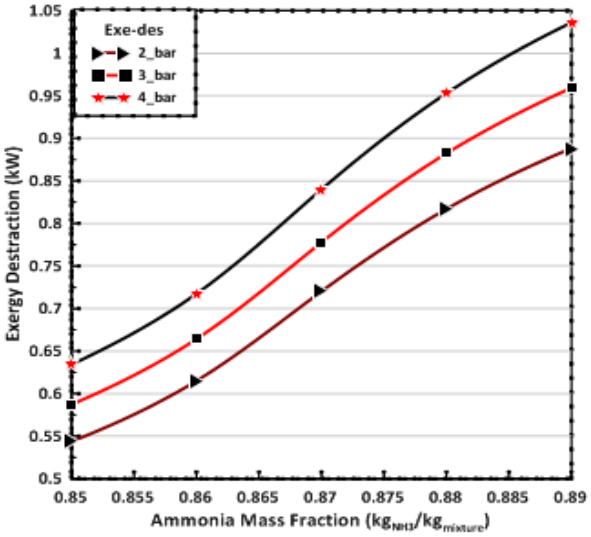


**Fig. (14): Exergy destruction of RGKCS at Pmax=35 bar and DF=0.3**

## 4. Conclusions

This study on a regenerative Kalina cycle system yielded several key findings:

1. Increasing ammonia mass fraction decreases thermal efficiency.
2. Increasing ammonia mass fraction increases net power output.
3. Increasing ammonia mass fraction decreases exergy efficiency.
4. The heat recovery vapor generator (HRVG) has the highest exergy destruction at around 48%.
5. Other significant exergy destructions are in the absorber (12%), separator (9%), and heat exchanger (8%).
6. Overall exergy destruction rises with increasing ammonia mass fraction due to higher circulation rates.

The experimental analysis shows trade-offs between efficiency and power output as ammonia concentration increases. The HRVG accounts for nearly half of the overall exergy destruction. The results quantify the sources of irreversibility in the cycle and the impacts of changing ammonia concentration. This provides insights to guide optimization of the regenerative Kalina cycle system.

Open Access
Vol. 14, No. 4, December 2024, pp. 154-169
P- ISSN: 2220-5381
E- ISSN: 2710-1096

## Nomenclature

| Symbol | Description |
|---|---|
| $\dot{E}_{in}$ | Exergy delivered by the source (kJ) |
| $\dot{W}_P$ | Power consumed by pump (kW) |
| $\dot{W}_T$ | Power produced by turbine(kW) |
| $\dot{W}_{net}$ | The net power(kW) |
| $\dot{m}_0$ | Output mass flow rate (kg/s) |
| $\dot{m}_i$ | Input mass flow rate (kg/s) |
| $\dot{m}$ | Mass flow rate (kg/s) |
| h | Specific enthalpy (kJ/kg) |
| $T_0$ | Surrounding temperature (°K) |
| **Greek Symbol** | |
| $(\eta_t)_{isent}$ | The isentropic efficiency of turbine |
| $(\eta_p)_{isent}$ | The isentropic efficiency of pump |
| η | Efficiency (%) |
| $\epsilon$ | Effectiveness |
| **Subscripts** | |
| th | thermal |
| ex | exergy |
| isen | isentropic |
| bp | Bubble point |
| H.G | Hot gases |
| tot | Total |
| **Abbreviations** | |
| AP | Approach point |
| DF | Dryness fraction (kg vapor of ammonia/kg total mass of vapor) |
| HRVG | Heat recovery vapor generator |
| LCV | Lower calorific value (kJ/kg) |
| $NH_3$-$H_2O$ | Ammonia-water |
| ORC | Organic Rankine Cycle |
| PP | Pinch point |
| RC | Rankine Cycle |
| RKC | Rankine-Kalina Combined cycle |
| TTD | Terminal temperature difference |

Open Access
Vol. 14, No. 4, December 2024, pp. 154-169
P- ISSN: 2220-5381
E- ISSN: 2710-1096

## References

[1] G. R. da Costa Horta, E. P. B. Júnior, L. F. Moreira, F. R. P. Arrieta, and R. N. de Oliveira, "Comparison of Kalina cycles for heat recovery application in cement industry", *Applied Thermal Engineering*, vol. 195, p. 117167, 2021. https://doi.org/10.1016/j.applthermaleng.2021.117167

[2] S. D. Parvathy and J. Varghese, "Energy analysis of a Kalina cycle with double turbine and reheating", *Materials Today: Proceedings*, vol. 47, pp. 5045-5051, 2021. https://doi.org/10.1016/j.matpr.2021.04.636

[3] F. I. Abam, T. A. Briggs, O. E. Diemuodeke, E. B. Ekwe, K. N. Ujoatuonu, J. Isaac, and M. C. Ndukwu, "Thermodynamic and economic analysis of a Kalina system with integrated lithium-bromide-absorption cycle for power and cooling production", *Energy Reports*, vol. 6, pp. 1992-2005, 2020. https://doi.org/10.1016/j.egyr.2020.07.021

[4] H. Ghaebi and H. Rostamzadeh, "Performance comparison of two new cogeneration systems for freshwater and power production based on organic Rankine and Kalina cycles driven by salinity-gradient solar pond," *Renewable Energy*, vol. 156, pp. 748-767, 2020. https://doi.org/10.1016/j.renene.2020.04.043

[5] H. R. Abbasi and H. Pourrahmani, "Multi-criteria optimization of a renewable hydrogen and freshwater production system using HDH desalination unit and thermoelectric generator", *Energy Conversion and Management*, vol. 214, p. 112903, 2020. https://doi.org/10.1016/j.enconman.2020.112903

[6] Y. Cao, H. A. Dhahad, T. Parikhani, A. E. Anqi, and A. M. Mohamed, "Thermo-economic evaluation of a combined Kalina cycle and humidification-dehumidification (HDH) desalination system integrated with thermoelectric generator and solar pond", *International Journal of Heat and Mass Transfer*, vol. 168, p. 120844, 2021. https://doi.org/10.1016/j.ijheatmasstransfer.2020.120844

[7] M. M. Hossain, M. S. Hossain, N. A. Ahmed, and M. M. Ehsan, "Numerical Investigation of a modified Kalina cycle system for high-temperature application and genetic algorithm based optimization of the multi-phase expander's inlet condition", *Energy and AI*, vol. 6, p. 100117, 2021. https://doi.org/10.1016/j.egyai.2021.100117

[8] M. Kaczmarczyk, B. Tomaszewska, and L. Pająk, "Geological and thermodynamic analysis of low enthalpy geothermal resources to electricity generation using ORC and

Open Access
Vol. 14, No. 4, December 2024, pp. 154-169
P- ISSN: 2220-5381
E- ISSN: 2710-1096

Kalina cycle technology", *Energies*, vol. 13, no. 6, p. 1335, 2020. https://doi.org/10.3390/en13061335

[9] L. Cao, J. Wang, and Y. Dai, "Thermodynamic analysis of a biomass-fired Kalina cycle with regenerative heater", *Energy*, vol. 77, pp. 760-770, 2014. https://doi.org/10.1016/j.energy.2014.09.058

[10] M. Kaczmarczyk, B. Tomaszewska, and A. Operacz, "Sustainable utilization of low enthalpy geothermal resources to electricity generation through a cascade system," *Energies*, vol. 13, no. 10, p. 2495, 2020. https://doi.org/10.3390/en13102495

[11] E. Özahi and A. Tozlu, "Optimization of an adapted Kalina cycle to an actual municipal solid waste power plant by using NSGA-II method", *Renewable Energy*, vol. 149, pp. 1146-1156, 2020. https://doi.org/10.1016/j.renene.2019.10.102

[12] C. Öksel and A. Koç, "Modeling of a Combined Kalina and Organic Rankine Cycle System for Waste Heat Recovery from Biogas Engine", *Sustainability*, vol. 14, no. 12, p. 7135, 2022. https://doi.org/10.3390/su14127135

[13] A. K. Nassir and H. A. Shahad, "Effect of Operating Conditions on Modified Kalina Cycle Performance", *International Journal of Heat & Technology*, vol. 40, no. 5, pp. 1186-11952, 022. https://doi.org/10.18280/ijht.400509

[14] A. K. Nassir and H. A. Shahad, "Energy and Exergy Performance Analysis of Different Kalina Cycle Configurations", *International Journal of Heat & Technology*, vol. 40, no. 6, pp. 1454-1461, 2022. https://doi.org/10.18280/ijht.400613

[15] A. H. Salloom, O. A. Abdulrazzaq, S. Sadoon, and W. G. Abdulnaby, "A review of the geothermal potential hot spots in Iraq using geophysics methods", *Journal of Petroleum Research and Studies*, vol. 12, no. 1, pp. 51-69, 2022. http://doi.org/10.52716/jprs.v12i1.590